Supplementary material: Solitons and propagating domain-walls in topological resonator arrays

YAKIR HADAD,[1,2] VINCENZO VITELLI,[3] AND ANDREA ALU[1,*]

[1]*Department of Electrical and Computer Engineering, The University of Texas at Austin, 1616 Guadalupe St., Austin, TX 78701, USA*
[2]*School of Electrical Engineering, Tel-Aviv University, Ramat-Aviv, Tel-Aviv, 69978, Israel*
[3]Instituut-Lorentz, Universiteit Leiden, 2300 RA Leiden, The Netherlands

**Corresponding author: alu@utexas.edu*

This text completes parts of the discussion in the main text regarding the soliton localization length, the definition of v_g, and the topological robustness to disorder and defects.

Localization length. The moving soliton solutions, as well as the stationary edge-states, share a similar scaling law as their intensity approaches $\boldsymbol{q = q_1^*}$. In order to see that we solve Eq. (4) in the main text under the assumption that $\boldsymbol{\alpha \approx \alpha_0 = Const}$, which is exactly true for the solitons associated with Fixed points 2, and 3, in the $\boldsymbol{|c| < v_g}$ case, or approximately true for the other solitons in the vicinity of $\boldsymbol{q_1^*}$. In this case, the solution to Eq. (4) reads

$$\frac{(\nu_0-\kappa)v_g\cos 2\alpha_0}{v_g^2-c^2}(\xi-\xi_0)= \ln\left|\frac{q}{q_0}\right|+\frac{\nu_0-\nu_\infty}{\nu_\infty-\kappa}\ln\left|\frac{(\nu_0-\kappa)+(\nu_\infty-\kappa)q}{(\nu_0-\kappa)+(\nu_\infty-\kappa)q_0}\right| \quad \text{(S1)}$$

where $q_0 = q(\xi_0)$. In the case that $\alpha_0 = \alpha_2^*, \alpha_3^*$ the solution is exact and Eq. (S1) becomes

$$\frac{(\nu_0-\kappa)}{\sqrt{v_g^2-c^2}}(\xi-\xi_0)= \ln\left|\frac{q}{q_0}\right|+\frac{\nu_0-\nu_\infty}{\nu_\infty-\kappa}\ln\left|\frac{(\nu_0-\kappa)+(\nu_\infty-\kappa)q}{(\nu_0-\kappa)+(\nu_\infty-\kappa)q_0}\right| . \quad \text{(S2)}$$

The solution (S2) exactly coincides with the static edge state solution that would be found if $c = 0$, along the blue and red trajectories in the phase portrait in Fig. 2 in the main text. This result confirms that the localization length of the solitons as well as of the static edge states is similar and thereby the intimate relation between them as also discussed for the mechanical case in Ref. [6] of the main text.

If the soliton "width" is $\Delta\xi$ then the temporal bandwidth of the soliton is given by

$$BW = \frac{|c|}{\Delta\xi} . \quad \text{(S3)}$$

For solitons A and B in the two cases $|c| < v_g$ and $|c| > v_g$ we can approximate $\Delta\xi$ by

$$\Delta\xi = \frac{2(\alpha_p-\alpha_0)}{-F(q(\alpha_p))[c+v_g\sin\alpha_p]} . \quad \text{(S4)}$$

This approximation has been carried out based on Eqs. (7-8) together with Eq. (4) in the main text.
For solitons C and D in the case $|c| < v_g$ we can approximate $\Delta\xi$ by

$$\Delta\xi = \frac{q_1^*-q_{2,3}^*}{F(q_a)q_a v_g\cos 2\alpha_{2,3}^*} \rightarrow \Delta\xi = \frac{2}{F(q_1^*/2)\sqrt{v_g^2-c^2}} , \quad \text{(S5)}$$

where $q_a = (q_1^*+q_2^*)/2$. The last two results yield the scaling length estimation given in the main text for the solitons width.

The meaning of $\boldsymbol{v_g = \kappa\Delta}$. The maximal group velocity of a linear SSH chain with coupling coefficients $\boldsymbol{\kappa}$ and $\boldsymbol{\nu_0}$ is given by $\boldsymbol{\max_{\varphi\in 1BZ} v_g = \Delta\min\{\nu_0,\kappa\}}$ which implies that in our case since we assume $\boldsymbol{\nu_\infty < \kappa < \nu_0}$ the maximal group velocity we expect in the linear limit of our chain (low intensities) is given by

$$v_g = \kappa\Delta . \quad \text{(S6)}$$

Therefore, we conclude that the structure we study can support solitons that propagate slower or faster than the maximal group velocity in the low intensity case.

Energy conservation of solitons in the discrete equation. Here we show that the soliton solutions we find in the main text conserve energy. We assume that the solutions are of Eq. (1) in the main text and that they satisfy the solution ansatz in Eq. (3) in the main text where $b_n^{(1,2)}$ are real. For that, we define solution energy as in the main text

$$E = \sum_n\left[q_n^2 - q_1^{*2}\right] \quad \text{(S7)}$$

Then, we calculate the derivative of E in time,

$$\frac{dE}{dt}=\frac{d}{dt}\sum_n\left[q_n^2-q_1^{*2}\right]=\sum_n \dot{q}_n^2=\sum_n\frac{d}{dt}\left(a_n^{(1)}a_n^{(1)*}+a_n^{(2)}a_n^{(2)*}\right)$$

$$=\sum_n\left(\dot{a}_n^{(1)}a_n^{(1)*}+\dot{a}_n^{(2)}a_n^{(2)*}\right)+c.c=2\,\mathrm{Re}\sum_n\left(\dot{a}_n^{(1)}a_n^{(1)*}+\dot{a}_n^{(2)}a_n^{(2)*}\right)$$

$$=-2\,\mathrm{Im}\sum_n\left(-j\dot{a}_n^{(1)}a_n^{(1)*}-j\dot{a}_n^{(2)}a_n^{(2)*}\right)=-2\,\mathrm{Im}\sum_n\left(\omega_0\,|\,a_n^{(1)}\,|^2+\right.$$

$$\left.\nu(q_n)a_n^{(2)}a_n^{(1)*}+\kappa a_{n-1}^{(2)}a_n^{(1)*}+\omega_0\,|\,a_n^{(2)}\,|^2+\nu(q_n)a_n^{(1)}a_n^{(2)*}+\kappa a_{n+1}^{(1)}a_n^{(2)*}\right)$$

$$=2\kappa\sum_n\left(b_{n+1}^1b_n^{(2)}-b_{n-1}^{(2)}b_n^{(1)}\right)=0$$

In the derivation above we use the fact the solution is of the discrete system in Eq. (1) of the main text (namely, without using the continuum limit approximation), and we use the solution ansatz in Eq. (3) of the main text, saying that the two resonators amplitude in each dimer have phase lag of 90deg with respect to each other. Then, we obtain that the solution is conservative, namely, its energy is time invariant and therefore the soliton does not lose energy during propagation even in the discrete limit.

Robustness against defects – Further discussion. Robustness against defects has been demonstrated in Fig. 5 of the main text and discussed there. Here we include additional results to complete the discussion, and provide further insights.

The response to a defect of fast soliton B with velocity $\boldsymbol{c=6\times10^{-3}}$ (same velocity as of fast soliton A shown in the main text) is shown in Fig. S1. Here, the defect in the linear bond is $\boldsymbol{\kappa_D=0.2\kappa}$, much stronger than the one used in the main text. Nevertheless, the shape of the soliton is completely preserved as it hits the defect, as shown in Fig. S1(a) and (b). Upon hitting the defect, the fast soliton becomes somewhat slower, as evident from the fact that the intensity hole becomes shallower [Fig. S1 (a)]. This means that it loses kinetic energy, which is transferred to scattered modes. A particular mode to mention, which may be excited after the interaction between the fast soliton and the strong defect, is an edge state. This edge state decays to a nonzero plateau level through the array, as predicated by the slow soliton phase space diagram in Fig. 2a. The edge state is clearly seen in Fig. S2, where we show the full scale of Fig. S1(a). The edge state is not excited if the defect is much weaker, as in Fig. 5 in the main text.

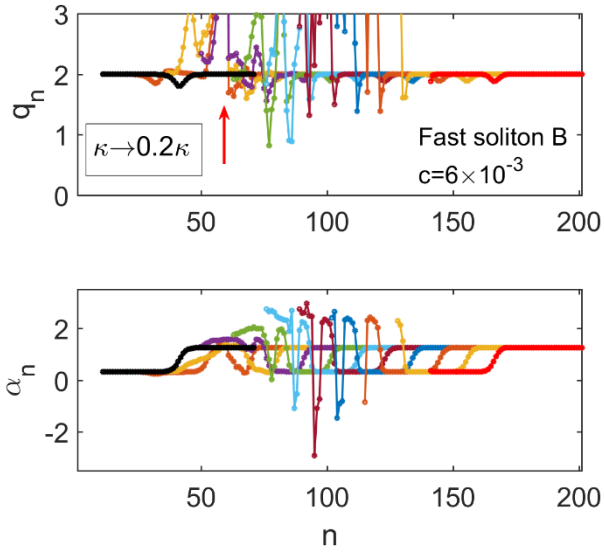

Fig. S1. Scattering of fast soliton B. Defect located at cell number 60. $\boldsymbol{\kappa_D=0.2\kappa}$. Despite the major defect the soliton preserves its shape as evident by comparing the black and red curves that correspond to the soliton before and sufficiently after the impact.

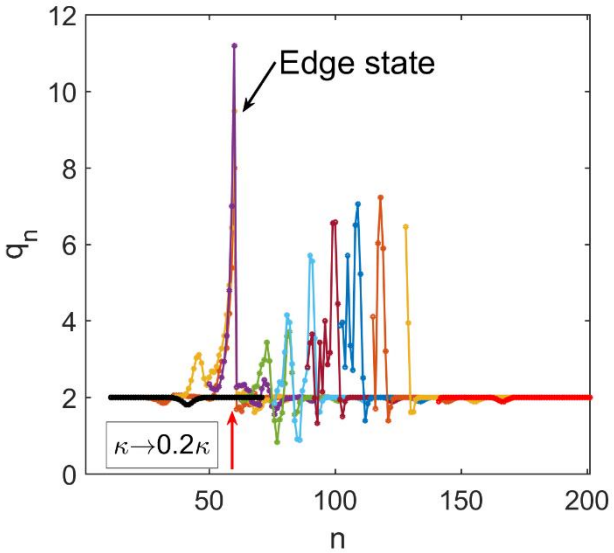

Fig. S2. Full scale image of Fig. S1(a). Here, the excitation of an edge state at the defect location is clear. This edge state is a result of the very strong defect. With a weaker defect of $\boldsymbol{\kappa\to0.75\kappa}$ (as used in the main text) it will not be excited.

We show in Fig. S3 the scattering simulation of fast soliton A along an array with a stronger defect. This is essentially the same data as in Fig. 5c and 5d, but with $\boldsymbol{\kappa_D=0.2\kappa}$. As for fast soliton B, the strong defect results in the excitation of an edge state at the defect location. The soliton here loses more of its kinetic energy compared to the case of a weaker defect considered in the main text. Consequently, it slows down further, as evident from the fact that it becomes sharper and taller compared to Fig. 5c. As for fast soliton B, the major defect yields the excitation of an additional edge state.

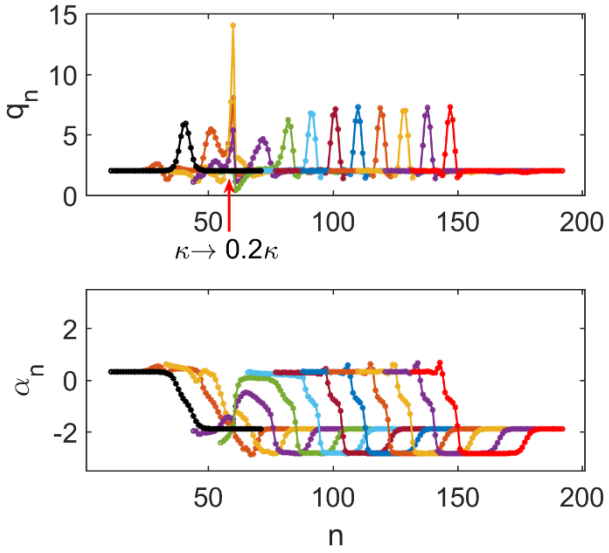

Fig. S3. Scattering of fast soliton A by a defect with $\boldsymbol{\kappa_D=0.2\kappa}$.

These results highlight how fast solitons A and B are quite robust. But what is the defect threshold above which this protection vanishes?

Clearly, for $\boldsymbol{\kappa_D = 0}$ no transmission can take place. Therefore, there has to be a transition after which the robustness is lost. In order to demonstrate this effect, we show in Fig. S4(a) and (b) the scattering dynamics of fast soliton A by a defect with $\boldsymbol{\kappa_D = 0.05\kappa}$. In this case, the topological protection is not sufficient, and fast soliton A is converted to fast soliton B, with a slower velocity $\boldsymbol{5.4\times10^{-3}}$, rather than $\boldsymbol{5.6\times10^{-3}}$, as found for the actual velocity of fast soliton A in Fig. 4c. The full scale of Fig. S4(a) is shown in Fig. S5. A strong edge state excitation is evident. Thus, we may conclude that, given certain initial soliton properties, upon hitting a defect, the stronger the defect, the more dominant the edge state excitation will be.

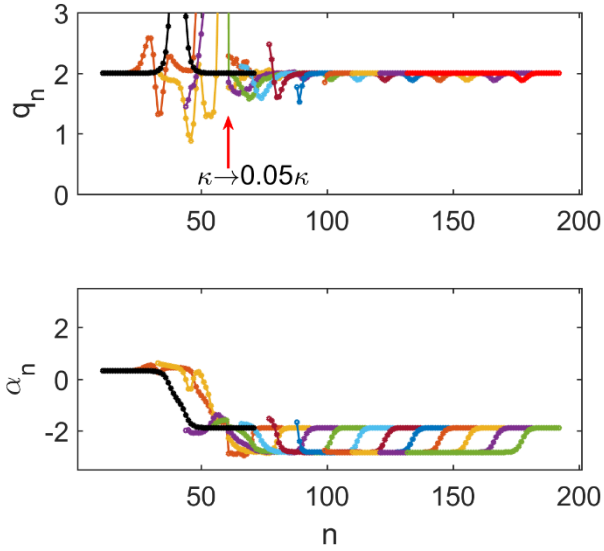

Fig. S4. Fast soliton A with $\boldsymbol{c = 6\times10^{-3}}$ imping a defect with $\boldsymbol{\kappa_D = 0.05\kappa}$.

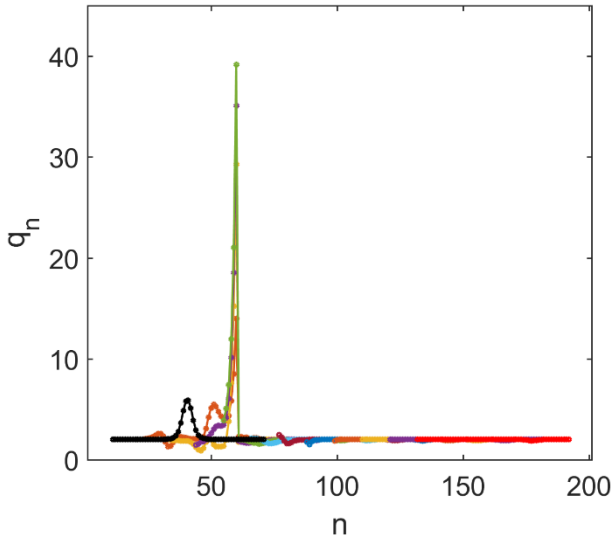

Fig. S5. Full scale of Fig. S4(a).

Finally, we demonstrate the robustness of fast soliton A against a widely distributed defect. In this case, the defect is located not only over a single cell, but over a *region* of cells between dimer 50 and dimer 75. The defects are random in both space and time, namely, they change randomly with time during the soliton propagation, maximizing the effect of randomness, and making stable propagation more challenging. The defected linear bond at cell number $\boldsymbol{n}$ is given by $\boldsymbol{\kappa_D(n,t)}$, which is a random function uniformly distributed in the range $\boldsymbol{[0.2\kappa, \kappa]}$. A careful observation reveals that the impinging soliton is transmitted and converted into two fast solitons of type A and B. However, the total transmitted topological charge is perfectly preserved, as evident from Fig. S6.

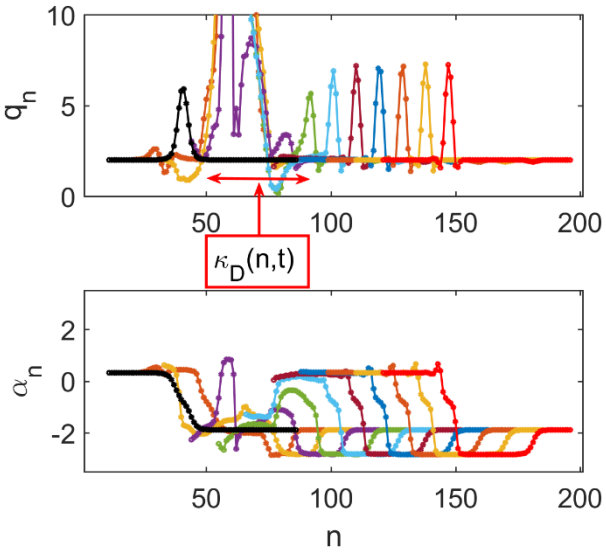

Fig. S6. Scattering of fast soliton A by a collection of random defects in both space and time. All the bonds between cell number 50 and number 75 are defected. The defect is random in space and time, uniformly distributed in the range $\boldsymbol{\kappa_D(n,t) \sim U[0.2\kappa, \kappa]}$.